9º Congresso Brasileiro de Engenharia de Fabricação
Joinville, Santa Catarina, Brasil

DEVELOPMENT OF CERIUM BASED CONVERSION COATINGS FOR CORROSION PROTECTION OF AZ91D MAGNESIUM ALLOY

Eloana Patrícia Ribeiro, eloana.ribeiro@ufabc.edu.br[1]
Renato Altobelli Antunes, renato.antunes@ufabc.edu.br[1]

[1]Universidade Federal do ABC (UFABC), CECS, Av. Dos Estados, 5001, Santo André – SP, 09210-580

Abstract*. The aim of the present work was to develop cerium conversion coatings on the surface of the AZ91D magnesium alloy. The converted layers were produced upon immersion in cerium nitrate solution at room temperature for different times (10 s, 20 s, 30 s, 60 s and 120 s). Surface morphology was examined using scanning electron microscopy (SEM).The surface chemical composition of the cerium-based films was determined by x-ray photoelectron spectroscopy (XPS) analyses. The effect of the treatment time on the corrosion resistance of the coated AZ91D alloy was assessed by electrochemical impedance spectroscopy (EIS) and potentiodynamic polarization using a 3.5 wt.% NaCl solution at room temperature as the electrolyte. The results revealed that the cerium films presented several microcracks and exfoliated regions. Nodular agglomerates were mainly formed on the specimens treated for long times (60 s and 120 s).The cerium content was not directly related to treatment time. The best corrosion resistance was observed for the specimens treated for 20 s.*

Keywords*: AZ91D alloy, cerium conversion coating, XPS.*

1. INTRODUCTION

Magnesium alloys are attractive materials for aeronautic, automotive, electronics and biomedical industries due to attributes such as low density, good electromagnetic shielding, high strength-to-weight ratio and good machinability (LIU *et al*., 2015; PHUONG *et al*., 2013; GRAY *et al*., 2002). Automotive industry is mainly interested in magnesium alloys as alternative materials to reduce vehicles weight. (CASTANO *et al*., 2012; MADDELA *et al*., 2010; MADDELA *et al*., 2012). In spite of their suitable profile for many industrial applications, magnesium alloys have high chemical reactivity and low electrochemical potential, resulting in high corrosion susceptibility. As a consequence, widespread use in several environments is prevented. (MADELLA *et al*., 2012).

Mg-Al alloys (AZ grade) are the most commonly used magnesium-based materials due to the low manufacturing cost, good mechanical properties and reasonable corrosion resistance. The microstructure of AZ alloys is characterized by the presence of α-Mg matrix and the intermetallic β-$Mg_{17}Al_{12}$ phase. By increasing the aluminum concentration the corrosion resistance is improved. This effect is due to the reduced β phase fraction for low Al contents, enhancing its cathodic character with respect to the magnesium matrix and accelerating the overall corrosion rate of the alloy. Na opposite effect is expected if the β-phase volume fraction is high for which it will act as na anodic barrier to the corrosion process (PARDO *et al*., 2008).

Despite the improved corrosion resistance associated with increasing volume fraction of the β-$Mg_{17}Al_{12}$ phase, corrosion mitigating strategies are still demanded to increase the service life of Mg-Al alloys. Surface coatings play a prominent role in this scenario. The coating protection efficiency is related to its homogeneity, compactness, adhesion to the substrate and self-repairing ability. Magnesium alloys can be protected by anodizing, organic films, chemical vapor deposition, electrodeposition and conversion coatings (GRAY *et al*., 2002).

Conversion coatings are easily produced at a low cost. The converted layers consist of oxides formed on the surface of the metallic substrate by immersing it in proper electrolytes. The coatings can be obtained either by chemical or electrochemical treatment. The electrolytes for conversion coatings can be based on chromates, phosphates or rare earth-based compounds. Chromates are the most common compounds. However, due to the toxicity associated with chromates, these compounds, are currently being replaced by less aggressive species (GRAY *et al*., 2002).

Harvey (HARVEY, 2013) reported that cerium has superior corrosion resistance with respect to other rare-earth elements such as neodymium, praseodymium, yttrium and lanthanum. Cerium oxide is non-carcinogenic and has large applicability as catalyst, abrasive, biomaterial and for corrosion protection purposes (CASTANO *et al*., 2015). Research devoted to cerium-based conversion coatings has increased recently aiming at studying their formation mechanism, morphology and corrosion resistance (BAI *et al*., 2007; CASTANO *et al*, 2014; JIANG *et al*., 2015; WANG *et al*., 2013).

In this context, the aim of the present work was to develp cerium converison coatings on the AZ91D magnesium alloy by immersion in cerium nitrate-based solutions. The converted layers were studied with regards to their corrosion resistance, surface morphology and chemical composition.

2. EXPERIMENTAL PROCEDURE

2.1 Material, surface preparation and conversion coating procedure

The substrate for the surface treatment was a AZ91D magnesium alloy ingot (wt.% 9.00 – 9.03 % Al; 0.65 – 0.70 % Zn; 0.23 – 0.27% impurities; Mg bal.) (BAGALÀ *et al*., 2012; WANG *et al*., 2009). The material was kindly provided by Rima Industrial Magnésio S/A and was employed in the as-cast condition. The specimens for the coating process were obtained by cutting the as-received ingot into small rectangular pieces with approximate dimensions 7 x 6 x 5 mm. A copper wire was connected at one face of the specimen using a conductive silver colloidal suspension in order to provide electrical contact for the corrosion tests. Next, the specimens were embedded in cold curing epoxy resin. After curing, surface preparation consisted of grinding with SiC paper up to grit 2400. Following surface finishing, the specimens were cleaned with distilled water and dried in a warm air stream provided by a heat gun.

The conversion coatings were obtained in an electrolyte consisting of 0.05 M $Ce(NO_3)_3.6H_2O$ and 0.254 M H_2O_2 (30 wt.%) solution at room temperature. Hydrogen peroxide is added to accelerate the formation of cerium-based coatings (MADDELA *et al*., 2012). The converted films were formed by immersion for different times: 10 s, 20 s, 30 s, 60 s and 120 s. After the treatment, the specimens were dried in air.

2.2 Coating characterization

Coating morphology was examined using scanning electron microscopy (SEM – FEI Quanta 250). Surface analysis was carried out to evaluate film chemical composition by X-ray photoelectron spectroscopy (XPS). XPS analyses were performed using K-alpha ThermoFisher Scientific instrument operating with Al-kα radiation source. The cerium layer was subjected to point analysis. Survey spectra were acquired with X-ray spot radius of 400 μm. The binding energies were calibrated with respect to the reference C1s peak at 284.6 eV.

The electrochemical behavior of the cerium layers was investigated in a 3.5 wt.% NaCl solution at room temperature. A conventional three-electrode cell set-up was employed using a platinum wire as the counter-electrode, Ag/AgCl as reference and the cerium-coated AZ91D specimens as working electrodes. Uncoated specimens were also tested for comparison purposes. The tests consisted of an initial 1-h monitoring of the open circuit potential (OCP) in order to ensure a steady state condition. Next, electrochemical impedance spectroscopy measurements were carried out at the OCP in the frequency range from 100 kHz to 10 mHz with an amplitude of 10 mV and acquisition of 10 points per decade. Potentiodynamic polarization tests were, then, performed from -300 mV versus the OCP up to +0.5 $V_{Ag/AgCl}$ at a sweep rate of 1 mV.s-1. The tests were conducted in triplicate using a Autolab M101 potentiostat/galvnostat.

3. RESULTS AND DISCUSSION

3.1 Surface morphology

SEM micrographs of the AZ91D alloy with and without the cerium-based conversion coatings are shown in Fig. 1. The uncoated surface presents several grooves originated from grinding during surface preparation. The treated surfaces, in turn, clearly shows the presence of a surface film characterized by several cracks and some exfoliated regions. The formation of microcracks and exfoliated regions is apparently related to the treatment time, being enhanced for longer immersion periods in the conversion bath. Microcracks formation can be associated with stresses generated in the film during drying. As the stresses relieve microcracks and exfoliated areas arise (BAGALÀ *et al*., 2012). WANG *et al*. (2009) have observed that microcracks were formed on cerium-based conversion coatings produced on the AZ91D alloy. The film was mainly formed on the α phase rather on the less reactive β-$Mg_{17}Al_{12}$. Consequently, the film is thicker over the α phase due to its anodic character with respect to the β phase. Different growth rates can also give rise to stresses and, ultimately, microcracks in the film (SUN *et al*., 2015).

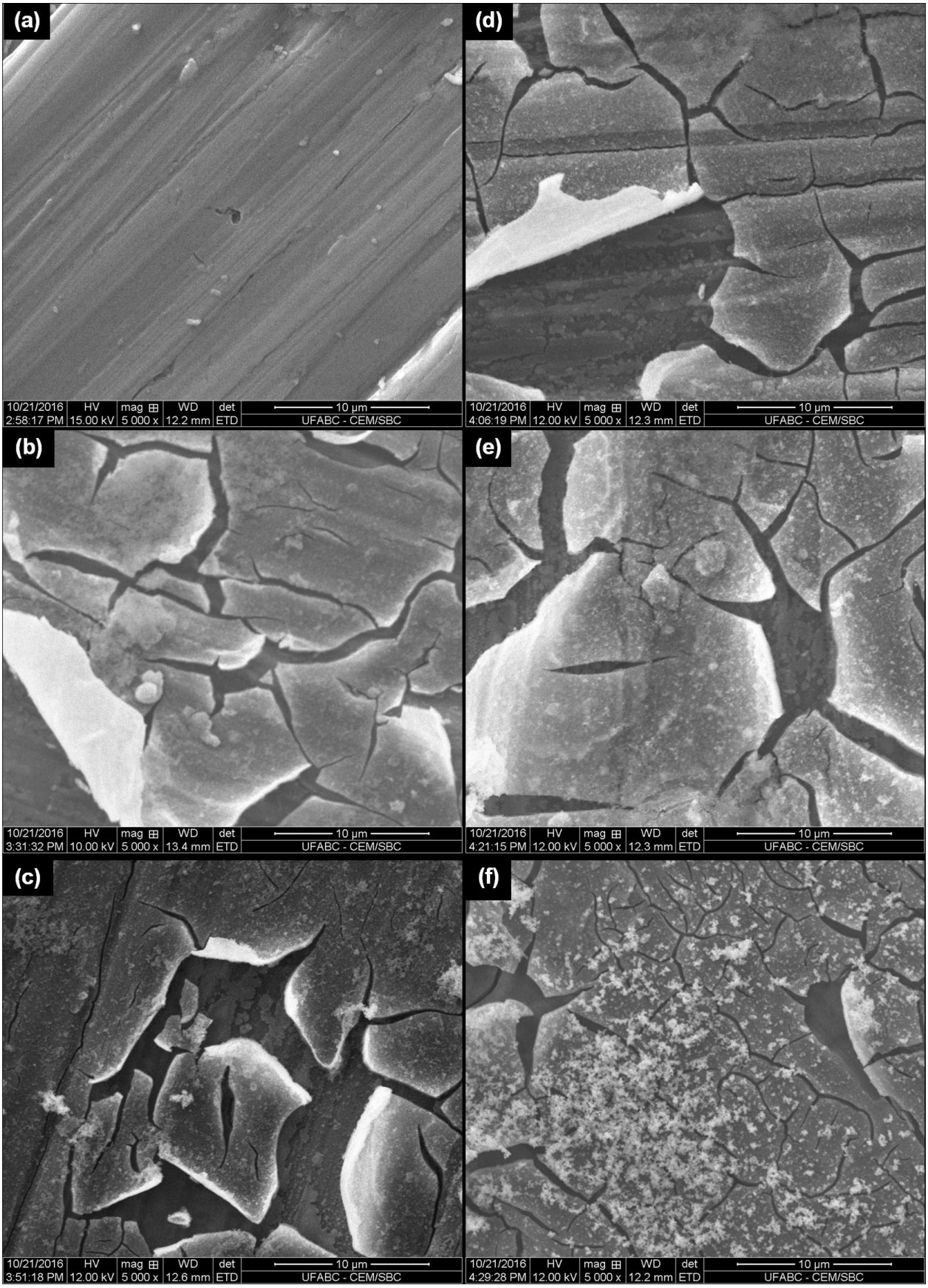

Figure 1. SEM micrographs of the AZ91D alloy: (a) uncoated; with conversion layers obtained at different deposition times: (b) 10; (c) 20; (d) 30; (e) 60 and (f) 120 seconds.

MADDELA *et al.* (2012) related increasing microcracks formation to a reduction of H_2O_2 concentration in the conversion bath. The density, morphology and size of microcracks are related to the dimensions of the cerium particles in the coating. According to MADDELA *et al.* (2010), homogeneous coatings are obtained for films with small cerium oxide particles evenly distributed within the converted layer. Microcracks size and distribution depend on the film thickness, being smaller and more homogeneously distributed for thick layers. Small microcracks can act as corrosion inhibitors since anodic regions become more uniform, reducing the overall corrosion rate. The coating can present a duplex structure, consisting of inner MgO-rich layer and outer Ce-rich layer. The film grows by the formation of the inner layer, followed by the development of the outer layer. Hydrogen evolution occurs around the α phase during the conversion treatment due to its high reactivity, entailing blisters formation which, in turn, can influence microcracking and exfoliation of the converted coating (MADDELA *et al.*, 2012; LEE *et al.*, 2013; SUN *et al.*, 2015).

In addition to the typical cracked aspect depicted above, the treated surfaces presented the formation of small nodular agglomerates above the cracked film. These nodules are most clearly seen for the longest treatment times as can be observed in Figs. 1e and 1f. Similar nodular formation has been reported by other authors. EDS analyses revealed their composition is mainly comprised of cerium oxides (SUN *et al.*, 2014; SUN *et al.*, 2015).

3.2 Surface analysis - XPS

XPS survey spectra of cerium coatings obtained at different treatment times are shown in Fig. 2. Cerium was detected in all the conversion coatings, independently of the treatment time, indicating successful incorporation of cerium upon immersion in the conversion bath. Ce3d peak reveals good coverage of the substrate surface by the conversion coating in agreement with the SEM micrographs shown in Fig. 1. Oxygen peaks were also detected. This is a common feature of cerium-based conversion coatings. Cerium oxides are formed during the treatment and the oxygen detected by XPS is related to their formation (LEI *et al.*, 2016). Magnesium peaks were also detected. The presence of magnesium also indicates that it is part of the conversion coatings. Some adventitious carbon was also detected and was ascribed to surface contamination.

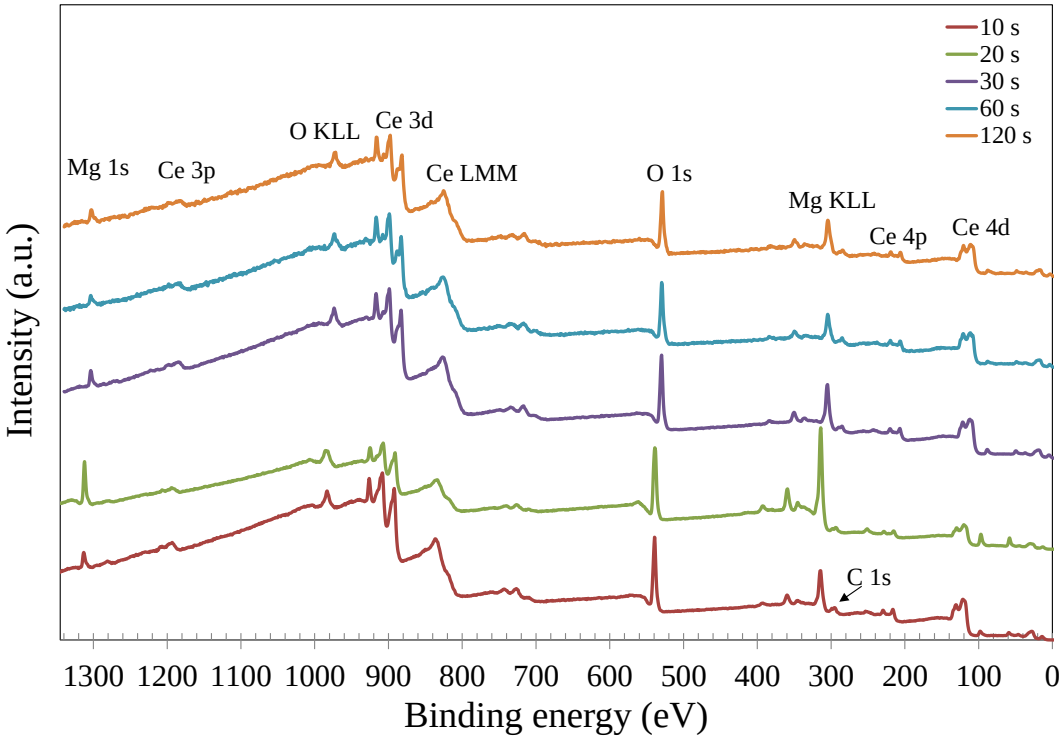

Figure 2. XPS survey spectra of cerium conversion coatings obtained at different treatment times.

The atomic percentage of each element was quantified with the Avantage software. The results are given in Fig. 3. The results indicate that, in spite of cerium incorporation for all the samples, it is not possible to observe direct correlation between the cerium concentration and the treatment time. The cerium content did not increase with time. Surface morphology was more affected by this parameter than the immersion conditions.

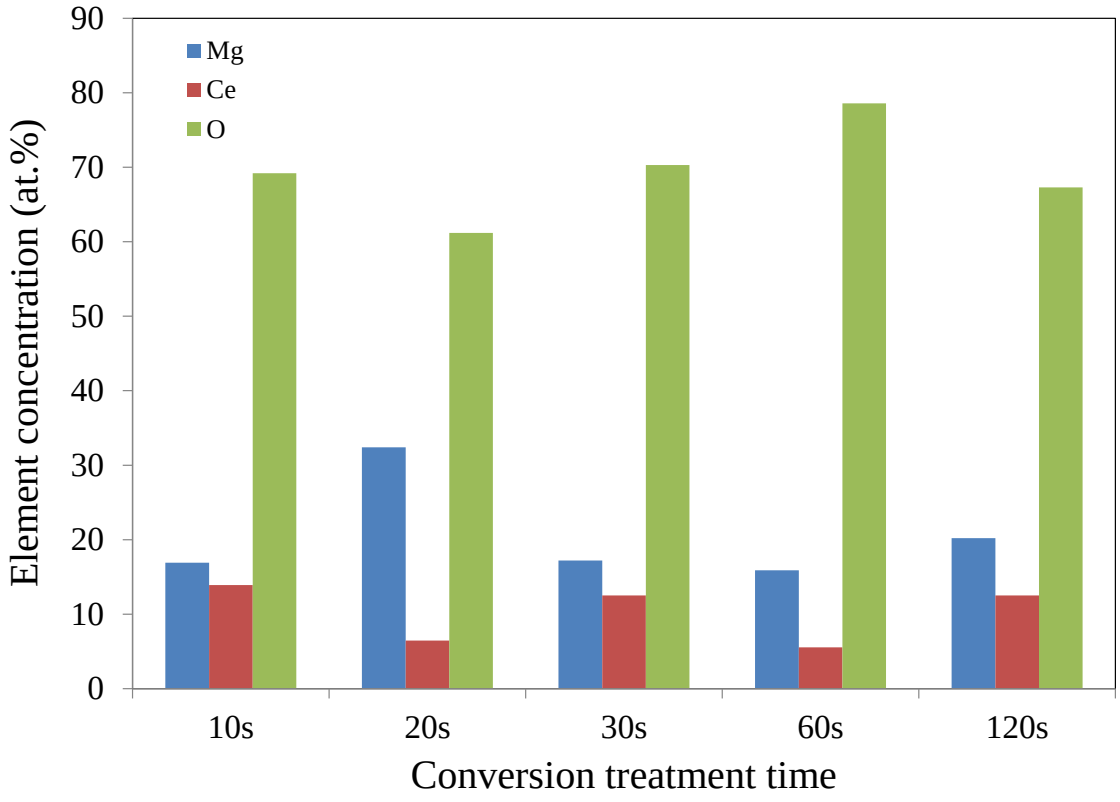

Figure 3. XPS atomic percentage at the surface of the cerium conversion coatings.

3.3 Electrochemical tests

3.3.1 EIS measurements

Nyquist plots obtained in 3.5 wt.% NaCl solution at room temperature for the AZ91D alloy in the uncoated condition and after conversion coating treatment in the cerium-based solution are shown in Fig. 4. The curves present similar shapes but different sizes, suggesting that corrosion mechanisms are the same whereas corrosion resistance depends on the treatment time. The plots are characterized by one capacitive loop at high to medium frequencies and an inductive loop at low frequencies. The capacitive loop is frequently associated with charge transfer reaction processes, denoting the corrosion behavior at the interface electrolyte/film. The low frequency inductive loop has been associated with the formation of adsorbed magnesium hydroxide layer of penetration of chloride ions, leading to pitting corrosion (GOBARA *et al*., 2015). This behavior is typical of magnesium alloys in aqueous electrolytes (BRETT *et al*., 2006; FANG *et al*., 2013; LIU *et al*., 2011). As is well-kown the capacitive loop diameter is associated with the corrosion resistance of the electrode surface (CHOI *et al*., 2016; ZUCCHINI *et al*., 2006). In this respect, the results point to a decrease of corrosion resistance for the coatings produced from 30 s up to 120 s of immersion. The best electrochemical behavior was obtained for the cerium film obtained at 20 s of immersion.

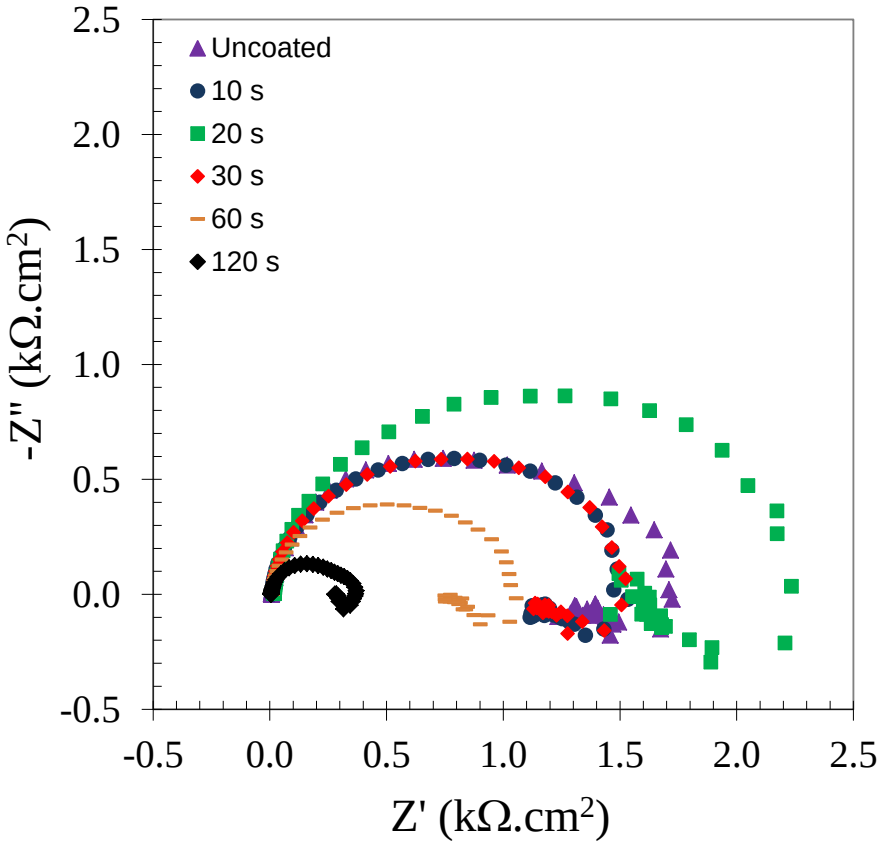

Figure 4. Nyquist plots for the AZ91D alloy in the uncoated condition and after conversion coating treatment in the cerium-based solution. Tests conducted in 3.5 wt.% NaCl solution at room temperature.

3.3.2 Potentiodynamic polarization

The electrochemical behavior of the AZ91D alloy was further characterized by potentiodynamic polarization. The polarization curves were obtained right after the EIS measurements and are displayed in Fig. 5. The values of corrosion potential (E_{corr}) and corrosion current density (i_{corr}) are shown in Tab. 1. They were obtained from the polarization curves by means of the Tafel extrapolation method, considering only the cathodic branches. E_{corr} is related to the corrosion probability of an electrode surface whereas i_{corr} is an indication of its corrosion rate (SUN *et al*., 2014).

The best corrosion resistance was achieved for the films obtained at 10 s and 20 s of immersion. Longer treatment times yielded an increased corrosion current density with respect to the uncoated substrate. The values of E_{corr} were nobler for the samples treated for 10 s and 20 s with respect to the pristine alloy but were little affected by the treatment time. These results are in agreement with those obtained by EIS. The improved corrosion resistance of magnesium alloys in the presence of cerium layers has been ascribed to an effective barrier effect of the film, decreasing electrolyte penetration into the substrate and avoiding the microgalvanic effect between α and β phases (WANG *et al*., 2009). In this respect, the treatment time has an obvious influence on the barrier efficiency of the converted layers which is progressively hampered as immersion surpasses 20 s. One can hypothesize that for longer times film porosity could increase due to an enhanced blistering formation during film formation, as a result of hydrogen evolution. Hence, compactness and homogeneity of the converted film would be favored for short treatment times.

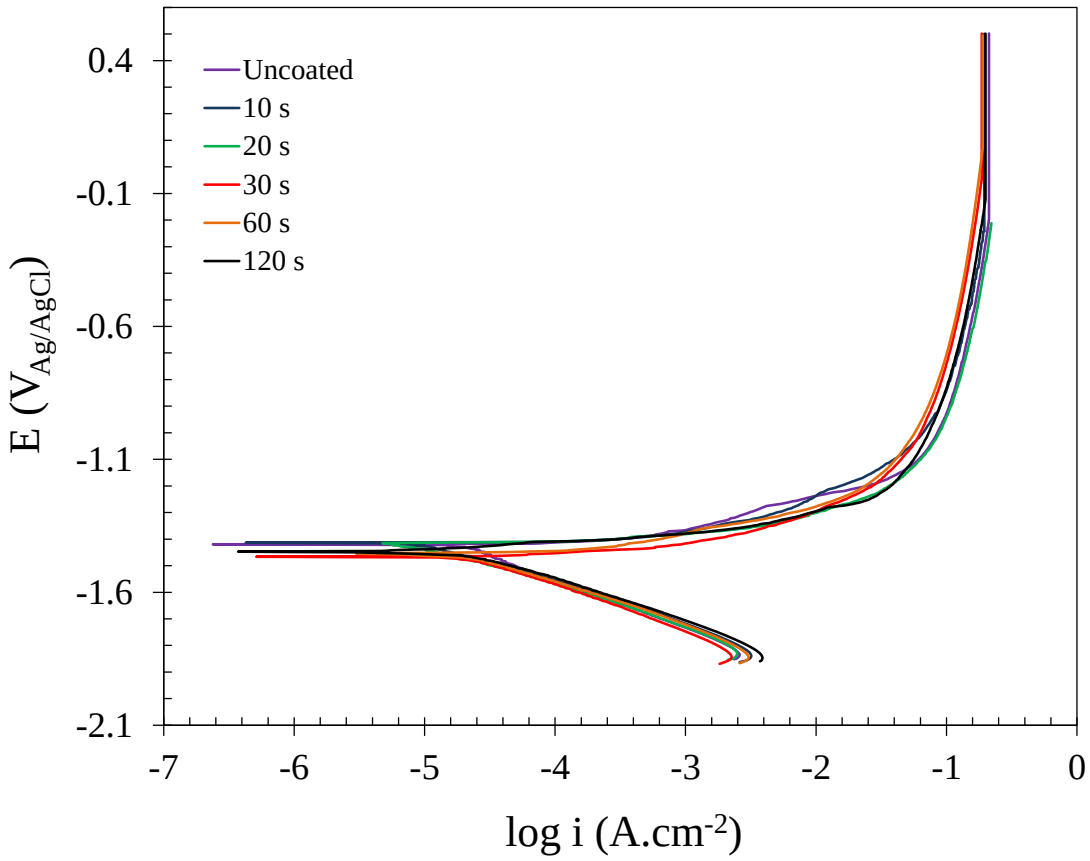

Figure 5. Potentiodynamic polarization curves for the AZ91D alloy in the uncoated condition and after conversion coating treatment in the cerium-based solution. Tests conducted in 3.5 wt.% NaCl solution at room temperature.

Table 1. Electrochemical parameters for the AZ91D alloy in the uncoated condition and after conversion coating treatment in the cerium-based solution

Sample	i_{corr} ($\mu A/cm^2$)	E_{corr} (V)
Uncoated	20.4	- 1.43
10 s	18.8	- 1.38
20 s	6.81	- 1.40
30 s	25.9	- 1.43
60 s	21.3	- 1.40
120 s	63.6	- 1.40

4. CONCLUSIONS

Cerium converison coatings were sucessfully obtained by immersion on the surface of the AZ91D magnesium alloy. The cerium layer is cracked and subjected to exfoliation. Surface morphology was affected by the treatment time. Some nodular agglomerates are observed for the longest immersion times. The surface chemical composition of the cerium coatings was determined by XPS analyses. The results revealed that cerium was incorporated after treatment, but its concentration was not affected by the immersion time. The corrosion resistance of the specimens treated for 20 s was higher than for the other conditions. This effect was rather due to morphological features than compositional aspects of the converted layer.

5. ACKNOWLEDGEMENTS

The authors are thankful to Capes for the financial support. Rima Industrial Magnésio S/A is acknowledged for kindly providing the AZ91D ingot used in the present work.

6. REFERENCES

BAGALÀ, P., LAMASTRA F. R., KACIULIS, S., MEZZI, A., MONTESPERELLI, G., 2012, "Ceria/stannate multilayer coatings on AZ91D Mg alloy", Surface & Coatings Technology, Vol. 206, pp. 4855–4863.

BAI, L., LI, DI., GUO, M., XIN, J., 2007, "Rare Earth Conversion Coating of Magnesium Alloy AZ91D", Materials Science Forum Vol. 546-549, pp 555-558.

BRETT, C. M. A., DIAS, L., TRINDADE, B., FISCHER, R., MIES, S., 2006, "Characterisation by EIS of ternary Mg alloys synthesized by mechanical alloying", Eletrochimica Acta, Vol. 51, pp 1752-1760.

CASTANO, C. E., MADDELA, S., O'KEEFEA, M. J., WANGB, Y. M., 2012, "A Comparative Study on the Corrosion Resistance of Cerium-Based Conversion Coatings on AZ91D and AZ31B Magnesium Alloys", CS Transactions, Vol. 41, pp. 3-12.

CASTANO, C. E., O'KEEFE, M. J., FAHRENHOLTZ, W. G., 2014, "Microstructural evolution of cerium-based coatings on AZ31 magnesium alloys", Surface & Coatings Technology Vol. 246, pp. 77–84.

CASTANO, C. E., O'KEEFE, M. J., FAHRENHOLTZ, W. G., 2015, "Cerium-based oxide coatings", Current Opinion in Solid State and Materials Science, Vol. 19, pp. 69–76.

CHOI, H. Y., KIM, W. J., 2016, "Development of the highly corrosion resistant AZ31 magnesium alloy by the addition of a trace amount of Ti", Journal of Alloys and Compounds, Vol. 664, pp 25-37.

FANG, D., LI, X., LI, H., PENG, Q., 2013, "Electrochemical Corrosion Behavior of Backward Extruded Mg-Zn-Ca Alloys in Different Media", Int. J. Electrochem. Sci., Vol. 8, pp 2551 – 2565.

GOBARA, M., SHAMEKH, M., AKID, R., 2015, "Improving the corrosion resistance of AZ91D magnesium alloy through reinforcement with titanium carbides and borides", Journal of Magnesium and Alloys, Vol. 3, pp 112-120.

GRAY, J. E., LUAN, B., 2002, "Protective coatings on magnesium and its alloys — a critical review", Journal of Alloys and Compounds, Vol.336, pp. 88–113.

HARVEY, T. G., 2013, "Cerium-based conversion coatings on aluminium alloys: a process review", Corrosion Engineering, Science and Technology, Vol. 48, pp. 248-269.

JIANG, X., GUO, R., JIANG, S., 2015, "Microstructure and corrosion resistance of Ce–V conversion coatingon AZ31 magnesium alloy", Applied Surface Science, Vol. 341, pp. 166–174.

LEE, Y. L., CHU, Y. R., CHEN, F. J., LIN, C. S., 2013, "Mechanism of the formation of stannate and cerium conversion coatings on AZ91D magnesium alloys", Applied Surface Science, Vol. 276, pp. 578– 585.

LEI, L., SHI, J., WANG, X., LIU, D., XU, H., 2016, "Microstructure and electrochemical behavior of cerium conversioncoating modified with silane agent on magnesium substrates", Applied Surface Science, Vol. 376, pp 161–171.

LIU, Y., WEI, Z., YANG, F., ZHANG, Z., 2011, "Environmental friendly anodizing of AZ91D magnesium alloy in alkaline borate–benzoate electrolyte", Journal of Alloys and Compounds, Vol. 509, pp 6440–6446.

LIU, B., ZHANG, X., XIAO, G., LU, Y., 2015, "Phosphate chemical conversion coatings on metallic substrates for biomedical application: A review", Materials Science and Engineering, Vol 47, pp 97–104.

MADDELA, S., O'KEEFE, M. J., WANG, Y. M., KUO, H. H., 2010, "Influence of Surface Pretreatment on Coating Morphology and Corrosion Performance of Cerium-Based Conversion Coatings on AZ91D Alloy ", CORROSION, Vol. 66.

MADDELA, S., O'KEEFE, M. J., WANG,Y. M., 2012, "Effect of Hydrogen Peroxide Concentration on Corrosion Resistance of Cerium-based Conversion Coatings on Mg AZ91D alloy", ECS Transactions, Vol. 41, pp. 13-26.

PARDO, A., MERINO, M. C., COY, A. E., ARRABAL, R., VIEJO, F., MATYKINA, E., 2008, "Corrosion behaviour of magnesium/aluminium alloys in 3.5 wt.% NaCl", Corrosion Science, Vol. 50, pp. 823–834.

PHUONG, N. V., LEE, K., CHANG, D., KIM, M., LEE, S., MOON, S., 2013, "Zinc Phosphate Conversion Coatings on Magnesium Alloys: A Review", Met. Mater. Int., Vol. 19, pp. 273-281.

SUN, J., WANG ,GG., 2014, "Preparation and corrosion resistance of cerium conversion coatings on AZ91D magnesium alloy by a cathodic electrochemical treatment", Surface & Coatings Technology, Vol. 254, pp. 42–48.

SUN, J., WANG, G., 2015, "Preparation and characterization of a cerium conversion film on magnesium alloy", Anti-Corrosion Methods and Materials,Vol.62, pp. 253–258.

WANG, C., ZHU, S., JIANG, F., WANG, F., 2009, "Cerium conversion coatings for AZ91D magnesium alloy in ethanol solution and its corrosion resistance", Corrosion Science, Vol.51 , pp. 2916–2923.

WANG, X., ZHUB, L., HEA, X., SUNA, F., 2013, "Effect of cerium additive on aluminum-based chemical conversion coating on AZ91D magnesium alloy", Applied Surface Science, Vol. 280, pp. 467– 473.

ZUCCHI, F., GRASSI, V., FRIGNANI, A., MONTICELLI, C., TRABANELLI, G., 2006, "Electrochemical behaviour of a magnesium alloy containing rare earth elements", Journal of Applied Electrochemistry, Vol. 36, pp. 195-204.

7. RESPONSIBILITY NOTICE

The authors are the only responsible for the printed material included in this paper.